THE JOURNAL OF BIOLOGICAL CHEMISTRY VOL. 286, NO. 49, pp. 42017–42026, December 9, 2011

Fluid Shear Stress and Sphingosine 1-Phosphate Activate Calpain to Promote Membrane Type 1 Matrix Metalloproteinase (MT1-MMP) Membrane Translocation and Endothelial Invasion into Three-dimensional Collagen Matrices*[S]

Received for publication, August 5, 2011, and in revised form, October 10, 2011 Published, JBC Papers in Press, October 14, 2011, DOI 10.1074/jbc.M111.290841

Hojin Kang[‡], Hyeong-Il Kwak[§], Roland Kaunas[‡], and Kayla J. Bayless[§1]

From the [‡]Department of Biomedical Engineering, Texas A&M University, College Station, Texas 77843 and [§]Department of Molecular & Cellular Medicine, Texas A&M Health Science Center, College Station, Texas 77843-1114

Background: Wall shear stress (WSS) and sphingosine 1-phosphate (S1P) combine to promote endothelial sprouting and angiogenesis.
Results: WSS and S1P activate calpains, and calpains are required for endothelial sprouting. Blocking calpains reduced membrane type-1 matrix metalloproteinase (MT1-MMP) membrane localization.
Conclusion: Calpains regulate MT1-MMP membrane localization.
Significance: These data uncover a new mechanism for controlling a key metalloproteinase in angiogenesis.

The vascular endothelium continually senses and responds to biochemical and mechanical stimuli to appropriately initiate angiogenesis. We have shown previously that fluid wall shear stress (WSS) and sphingosine 1-phosphate (S1P) cooperatively initiate the invasion of human umbilical vein endothelial cells into collagen matrices (Kang, H., Bayless, K. J., and Kaunas, R. (2008) *Am. J. Physiol. Heart Circ. Physiol.* 295, H2087–2097). Here, we investigated the role of calpains in the regulation of endothelial cell invasion in response to WSS and S1P. Calpain inhibition significantly decreased S1P- and WSS-induced invasion. Short hairpin RNA-mediated gene silencing demonstrated that calpain 1 and 2 were required for WSS and S1P-induced invasion. Also, S1P synergized with WSS to induce invasion and to activate calpains and promote calpain membrane localization. Calpain inhibition results in a cell morphology consistent with reduced matrix proteolysis. Membrane type 1-matrix metalloproteinase (MT1-MMP) has been shown by others to regulate endothelial cell invasion, prompting us to test whether calpain acted upstream of MT1-MMP. S1P and WSS synergistically activated MT1-MMP and induced cell membrane localization of MT1-MMP in a calpain-dependent manner. Calpain activation, MT1-MMP activation and MT1-MMP membrane localization were all maximal with 5.3 dynes/cm^2 WSS and S1P treatment, which correlated with maximal invasion responses. Our data show for the first time that 5.3 dynes/cm^2 WSS in the presence of S1P combine to activate calpains, which direct MT1-MMP membrane localization to initiate endothelial sprouting into three-dimensional collagen matrices.

Biochemical and mechanical stimuli promote angiogenesis and vascular remodeling. Angiogenesis is the formation of new blood vessels from pre-existing vessels and is required for development, wound healing, and pathological events (1–5). Endothelial cells (ECs)[2] in the vascular system must continually sense and respond to both biochemical and mechanical stimuli within their microenvironment to appropriately initiate angiogenesis. Proangiogenic factors such as sphingosine 1-phosphate (S1P), vascular endothelial growth factor (VEGF), and basic fibroblast growth factor are potent stimulators of new blood vessel growth (2, 6–8).

ECs can sense their hemodynamic environment (9, 10), and these forces can alter vascular structures (11–13). Increased capillary growth from sprouting vessels in frog larvae was observed with high flow, whereas capillaries regressed when flow ceased (14). The growth of microvessels in tumors is similarly responsive to flow (15). Experimental disruption of normal flow during development results in heart or vascular defects (16–19). Dickinson and colleagues (13) demonstrated that fluid shear stress is crucial for normal vascular remodeling during development. Thus, blood flow, like biochemical factors, is a strong regulator of microvascular development and remodeling.

Although biochemical signals that stimulate angiogenesis are well studied, signals downstream that integrate biochemical and hemodynamic signals to control new blood vessel growth are defined poorly. We previously reported that 5.3 dynes/cm^2

* This work was supported, in whole or in part, by National Institutes of Health Grant R01 HL09576 (to K. J. B.). This work was also supported by American Heart Association Scientist Development Grants 0530020N (to K. J. B.) and 0730238N (to R. K.).

[S] The on-line version of this article (available at http://www.jbc.org) contains supplemental Figs. 1–3.

[1] To whom correspondence should be addressed: 440 Reynolds Medical Bldg., Dept. of Molecular & Cellular Medicine, Texas A&M Health Science Center, College Station, TX 77843-1114. Tel.: 979-845-7287; Fax: 979-847-9481; E-mail: kbayless@medicine.tamhsc.edu.

[2] The abbreviations used are: EC, endothelial cell; WSS, wall shear stress; S1P, sphingosine 1-phosphate; MT1-MMP, membrane type matrix metalloproteinase-1; HUVEC, human umbilical vein endothelial cell; TIMP-1, tissue inhibitor of metalloproteinase-1; ALLN, *N*-Acetyl-Leu-Leu-Nle-CHO.

WSS acts synergistically with S1P to stimulate robust EC sprouting responses (23). In the present study, we use this three-dimensional invasion system to better define the combined influence of WSS and S1P on the initiation of sprouting angiogenesis where ECs transition from a quiescent to an invading phenotype.

Calpain is a plausible candidate for regulating the transition from a quiescent to an invasive phenotype. Various exogenous stimuli activate calpains, including WSS (24, 25) and VEGF (26). Calpains are intracellular calcium-activated cysteine proteases that regulate migration by cleaving talin, vinculin, paxillin, focal adhesion kinase, and cortactin (27–29). Calpain inhibitors block endothelial alignment in response to WSS (30), basic fibroblast growth factor-induced corneal angiogenesis (31), and Matrigel-induced angiogenesis *in vivo* (26). Calpains are required for cell spreading (28, 32, 33) and mediate membrane protrusion and cell movement in two-dimensional systems (34–37). Because calpain activity is modulated in ECs by growth factors and mechanical stimuli, we investigated the functional requirement for calpains in initiating EC sprouting events induced by WSS and S1P in three-dimensional collagen matrices. Importantly, the molecular events downstream of calpain activation that initiate angiogenesis are not completely defined.

MT1-MMP activation is a key event in angiogenic sprouting and invasion events. Membrane-type matrix metalloproteinases (MT-MMPs) function alongside integrins and growth factors to direct angiogenic sprouting and lumen formation (38–43). Mice lacking MT1-MMP have developmental delays, a reduced lifespan and defective sprouting responses (38, 45, 46). The MT1-MMP cytoplasmic tail is phosphorylated by Src to regulate proteolytic activity and membrane localization (47), and S1P stimulates translocation of MT1-MMP to the membrane (48). MT1-MMP is clearly required for vessel outgrowth and lumen formation (38, 39, 41, 42), but the intracellular molecular events that control MT1-MMP activation and membrane translocation following proangiogenic stimulation of ECs are defined incompletely. Here, we investigated whether calpain activation acts upstream of proangiogenic factor-induced MT1-MMP membrane translocation and activation. We demonstrate for the first time an ability of calpain to regulate MT1-MMP membrane localization in ECs following treatment with S1P and WSS.

EXPERIMENTAL PROCEDURES

Cell Culture—Unless otherwise indicated, all reagents were obtained from Sigma. Human umbilical vein endothelial cells (HUVECs) were purchased from Lonza BioProducts (San Diego, CA), maintained as described previously (49), and used at passage 4–6.

Shear Stress Experiments—The WSS system has been described previously in detail (23). Type I collagen was purified (50) and used to prepare collagen matrices at 3.75 mg/ml (51, 52) containing 1 μM D-*erythro*-sphingosine 1-phosphate (Avanti Polar Lipids). Silicone rubber membranes (Specialty Manufacturing, Inc.) containing eight perforated holes were adhered to 50 × 75 mm glass microscope slides to form circular wells 7 mm in diameter (118 μl/cm^2). Collagen matrices were allowed to polymerize within the wells for 30 min at 37 °C in a humidified 5% CO_2 incubator. EC monolayers (120,000 cells/cm^2) were allowed to attach to the collagen matrices for 60 min in perfusion medium consisting of M199 containing reduced serum supplement II (2 mg/ml BSA, 20 ng/ml human holotransferrin, 20 ng/ml insulin, 17.1 ng/ml sodium oleate, and 0.02 ng/ml sodium selenite) and 50 μg/ml ascorbic acid before being assembled into parallel plate flow chambers designed to apply uniform steady WSS to the cell monolayer. The WSS magnitude was calculated as $\tau = 6\mu Q/wh^2$, where τ is wall shear stress, μ is fluid viscosity (0.7 centipoise), Q is flow rate, w is the width of the flow channel (29.21 mm), and h is the height of the flow channel.

Calpain Inhibition Experiments—ALLN (10 μM, in ethanol) and calpain inhibitor III (50 μM in dimethyl sulfoxide) were obtained from Calbiochem. ECs were exposed to inhibitors 1 h prior to onset of WSS or S1P treatment and maintained in the perfusate for 18 h.

Calpain Activity Assays—Calpain activity was measured using the Calpain-Glo™ protease assay kit (Promega). Collagen matrices containing ECs were collected and incubated in extraction buffer containing 0.9% Triton X-100, 0.1 M phenylmethylsulfonyl fluoride, and 20 μg/ml aprotinin at 4 °C for 10 min. Samples were vortexed every 5 min and centrifuged for 10 min at 12,000 × *g* at 4 °C. Supernatants were collected and stored at −80 °C until use. The chemiluminescent reaction was initiated by combining the supernatant with Suc-LLVY-Glo™ substrate diluted 1:100 in assay buffer (luciferin detection reagent and Calpain-Glo™ buffer), mixed gently, and added to 96-well plates for measurement in a luminometer (Wallac 1420 Multilabel Counter, PerkinElmer Life Sciences). Western blot analyses were performed with antibodies directed to GAPDH to verify equal loading between samples. Experiments were performed three times in triplicate wells. Average values were recorded and plotted with S.D.

MT1-MMP Activation Assays—MT1-MMP (MMP-14) activity was measured according to the manufacturer's instructions using a SensoLyte™ 520 MMP-14 assay kit (Anaspec). The collagen matrices containing ECs were homogenized in assay buffer containing 0.1% Triton X-100 at 4 °C for 10 min and centrifuged for 10 min at 12,000 × *g* at 4 °C. Supernatants were collected and stored at −80 °C until use. Assay buffer and MMP-14 substrate (5-FAM/QXL ™520 FRET peptide) were warmed to room temperature. MMP-14 substrate was diluted 1:100 in assay buffer and then added to the supernatant. The reagents were mixed gently, added to 96-well plates, and measured for fluorescence intensity at excitation and emission wavelengths of 490 ± 20 nm and 520 ± 20 nm, respectively. Culture medium used for all experiments contained tissue inhibitor of metalloproteinase-1 (TIMP-1) to allow specific detection of MT1-MMP activation. Stable 293 cell lines expressing TIMP-1 were generated to produce TIMP-1-conditioned medium and are described in detail elsewhere.[3]

Western Blot Analyses—Protein lysates were collected in 1.5× Laemmli sample buffer and separated by SDS-PAGE

[3] H.-I. Kwak, H. Kang, E. A. Mendoza, S.-C. Su, S. A. Maxwell, and K. J. Bayless, submitted for publication.

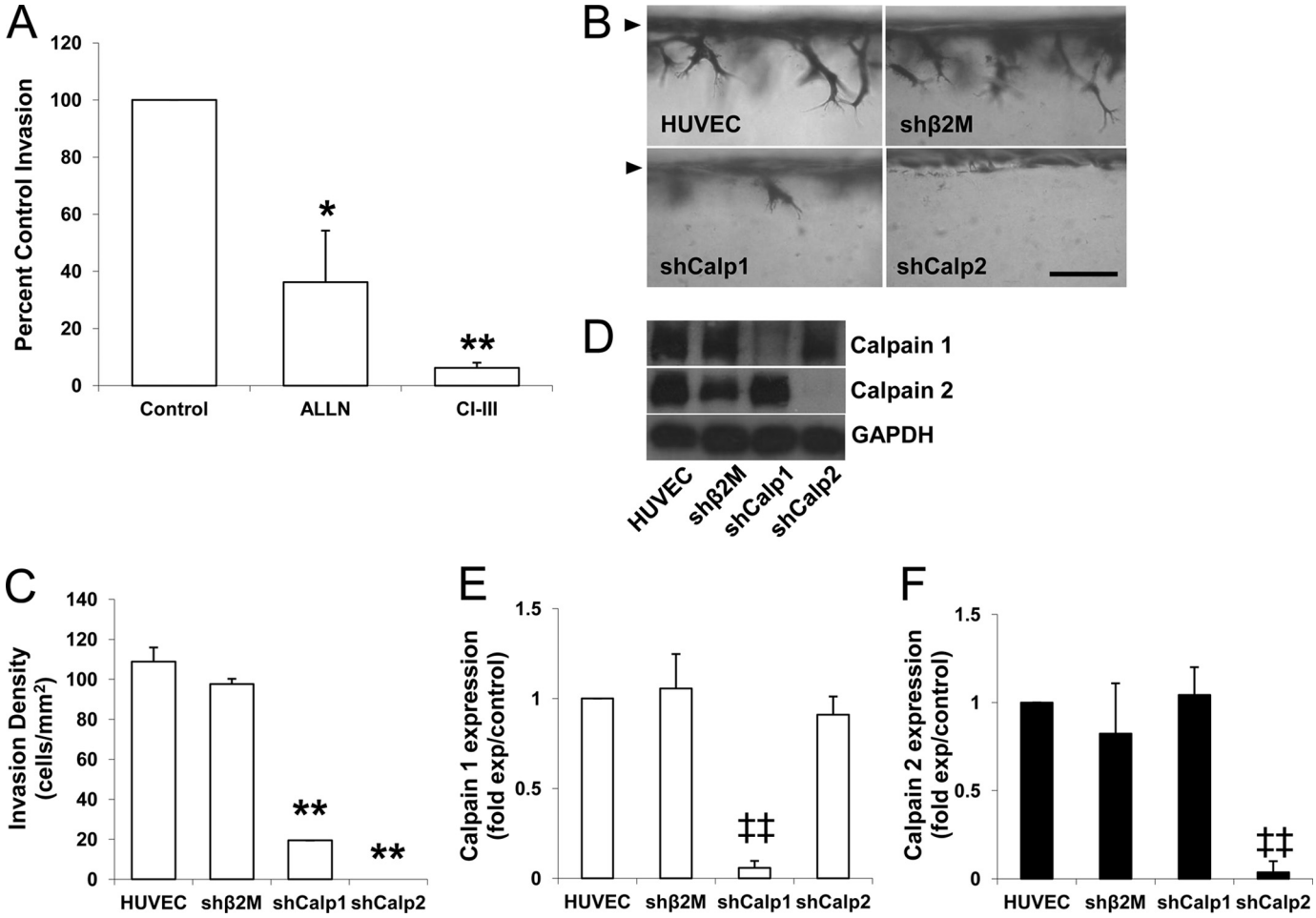

FIGURE 1. **Calpains are required for WSS- and S1P-induced EC invasion.** *A*, ECs were seeded on collagen matrices containing 1 μM S1P and treated with 5.3 dynes/cm^2 WSS with vehicle, 10 μM ALLN, or 50 μM calpain inhibitor III (*CI-III*) for 18 h. Cultures were fixed and stained to quantify the number of cells invading per field. Inhibitors were tested in three individual experiments (mean ± S.D., $n = 18$ fields), and data were normalized to control values. *B* and *C*, ECs transduced without (HUVEC) or with lentiviruses delivering shRNA directed to β2 microglobulin (*shβ2M*), calpain 1 (*shCalp1*), or calpain 2 (*shCalp2*) were stimulated with 1 μM S1P and 5.3 dynes (*dyn*)/cm^2 WSS for 24 h. Cultures were fixed and stained (*B*), and the invasion densities quantified for each condition from five individual experiments are summarized (*C*; mean ± S.D., $n = 21$ fields). *D*, culture extracts were immunoblotted with antibodies against calpain 1, 2, and GAPDH. *E* and *F*, the blots were quantified by densitometric analysis from three independent experiments (mean ± S.D.). *, $p < 0.05$ and **, $p < 0.01$ *versus* control or shRNA directed to β2 microglobulin treatment; ‡‡, $p < 0.01$ *versus* all others. *Scale bar*, 100 μm.

before being transferred to polyvinylidene fluoride membranes (Fisher Scientific). After blocking in 5% nonfat dry milk at room temperature for 1 h, the membranes were incubated with monoclonal antisera directed against GAPDH (1:10,000; Abcam) and polyclonal antisera directed against calpain 1 and 2 (1:2,000; Abcam), calpastatin (1:1,000; Cell Signaling), or MT1-MMP (1:2,000; Santa Cruz Biotechnology) at room temperature for 3 h. The membranes were washed three times in Tris-Tween 20 saline (150 mM sodium chloride, 2.5 mM Tris, 0.001% Tween 20) before incubation with rabbit anti-mouse secondary antibody or goat anti-rabbit secondary antibody (1:5,000; DAKO) in Tris-Tween 20 saline containing 5% milk for 1 h. Immunoreactive proteins were visualized using enhanced chemiluminescence (Millipore) and exposing the membranes to film (Denville Scientific). For image quantification, images were scanned with a FluorChem 8900 digital imaging system (Alpha Innotech, San Leandro, CA). Band intensities were measured using NIH ImageJ image analysis software.

Imaging and Analysis—Following each experiment, collagen matrices containing invading cells were washed briefly in PBS, fixed in 3% glutaraldehyde in PBS for 2 h, stained with 0.1% toluidine blue in 30% methanol for 12 min, and washed with water to clearly identify invading cells. To quantify invasion density, *en face* images were observed using bright-field illumination with a 10× objective on an Olympus BH-2 upright microscope. The microscope was focused on the invading cells, which were located immediately below the EC monolayer. Each data point represents a field in the center of a well where the number of invading cells was counted manually using an eyepiece equipped with an ocular grid covering an area of 1 mm^2. A single measurement was recorded for each well.

Cross-sectional digital images were collected using an Olympus CKX41 inverted microscope equipped with an Olympus Q-Color 3 camera. The invasion distance was measured for individual sprouts as the distance from the cell monolayer to the point of deepest penetration into the matrix. The nucleus penetration distance for individual sprouts was measured using the distance between the cell monolayer and the nucleus of the invading cell. Invasion diameter for individual sprouts was recorded as the cross-sectional width of the structure at its widest point.

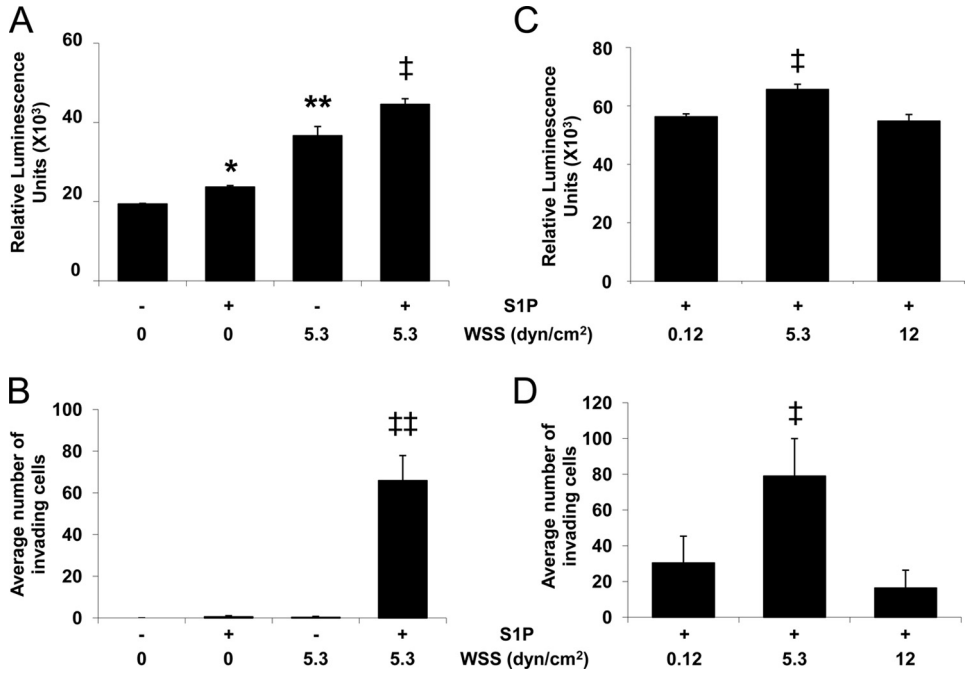

FIGURE 2. **S1P and 5.3 dynes/cm^2 WSS synergistically activate calpains and increase EC invasion.** EC monolayers seeded on collagen matrices were subjected to the indicated magnitudes of WSS in the absence or presence of S1P for 6 (*A* and *C*) or 18 h (*B* and *D*). The cultures were then either lysed to measure calpain activity (*A* and *C*) or used to quantify the average number of invading cells (*B* and *D*). As described under "Experimental Procedures," calpain activation was recorded as relative fluorescence units (mean ± S.D.; $n = 3$) using the Calpain-Glo™ protease assay kit. Western blot analyses were performed with antibodies directed to GAPDH to verify equal loading between samples (not shown). Each data point (mean ± S.D.) was derived by averaging band intensities from three experiments. *, $p < 0.05$ and **, $p < 0.01$ *versus* no S1P and no WSS treatment; ‡, $p < 0.05$ and ‡‡, $p < 0.01$ *versus* all other treatments. *dyn*, dynes.

Gene Silencing Using shRNA—shRNA constructs were purchased from Sigma-Aldrich and prepared from glycerol stocks for calpain 1 (SHCLNG-NM_005186), calpain 2 (SHCLNG-NM_007148), and β2 microglobulin (SHCLNG-NM_004048). Lentiviruses were generated in 25 cm^2 dishes as described previously (53) using 1.5 μg of backbone vector, 4.5 μg of ViraPower packaging mix (Invitrogen), and 12 μl of Lipofectamine 2000 (Invitrogen). Viral supernatants were harvested from 293FT cells at 48 h, passed through 0.45-μm filters (Millipore), and incubated with 4×10^5 ECs (passage 3) and polybrene (12 μg/ml). ECs were given fresh growth medium after 4 h. ECs expressing shRNA were selected with puromycin (0.2 μg/ml) for 2 weeks prior to invasion assays. Successful expression of mutant genes and protein silencing was confirmed by Western blot analyses.

Cell Transfection and Immunofluorescence Analyses—Collagen type I (20 μg/ml) was used to coat glass slides (75 × 50 × 1 mm) prior to transient transfections. Plasmid DNA (6 μg) expressing MT1-MMP, calpain 1 or calpain 2 fused to GFP, and 12 μl of Lipofectamine 2000 were diluted separately in 500 μl of Opti-MEM (Invitrogen) for 5 min and then combined for 20 min. Meanwhile, ECs were trypsinized, pelleted, and resuspended in 3 ml of DMEM with 20% FBS. Cell suspensions (1 ml) were incubated with the DNA/Lipofectamine complexes and seeded onto glass slides (2 h) before addition of 10 ml culture medium without antibiotics. The next day, cells were treated with various combinations of WSS and S1P as indicated and then fixed and imaged.

To quantify MT1-MMP-GFP localization to the cell periphery, outlined section of cells were manually traced in Adobe Photoshop, and the pixel intensity inside a 10-pixel-wide outline of the cell was quantified using ImageJ software. To avoid measuring fluorescence intensity from perinuclear staining, any perinuclear staining that entered the outline was excluded from the analysis. The cell fluorescence intensity histogram was normalized by setting the darkest cytoplasmic region in the cell to a pixel intensity of zero. The extent of MT1-MMP-GFP localization to the cell periphery was defined as the average pixel intensity within the analysis region. The quantification of MT1-MMP-GFP localization to the cell periphery was measured from three individual experiments ($n = 25$ cells).

Membrane Fractionation—Cells were seeded on glass slides overnight and treated with or without 1 μM S1P for 1 h prior to the application of the indicated levels of shear stress for an additional 2 h. Membrane fractions were prepared by incubating the cells in lysis buffer (20 mM HEPES, pH 7.4, 20 mM NaCl, 1.5 mM $MgCl_2$, 250 mM sucrose, 1 mM EDTA, 2 mM phenylmethylsulfonyl fluoride, and Complete Protease Inhibitor Mixture, Roche Diagnostics). Lysates were passed through a 27-gauge needle 10 times using a 1-ml syringe and kept on ice for 20 min. After homogenization, lysates were centrifuged at 1000 × *g* for 5 min at 4 °C to remove unbroken cells. The supernatant was removed and centrifuged at 150,000 × *g* for 30 min at 4 °C in a TL-100 ultracentrifuge (Beckman Instruments). The resulting supernatants contained cytoplasmic fractions. Pellets containing the membrane fractions were resuspended in lysis buffer with 0.5% Nonidet P-40.

Statistical Analysis—Data are presented as the mean ± S.D. for each group of samples. Statistical analyses were performed using SAS software (Cary, NC). Comparisons between two groups were performed using Student *t* tests. Comparisons between three or more groups were performed by one-way

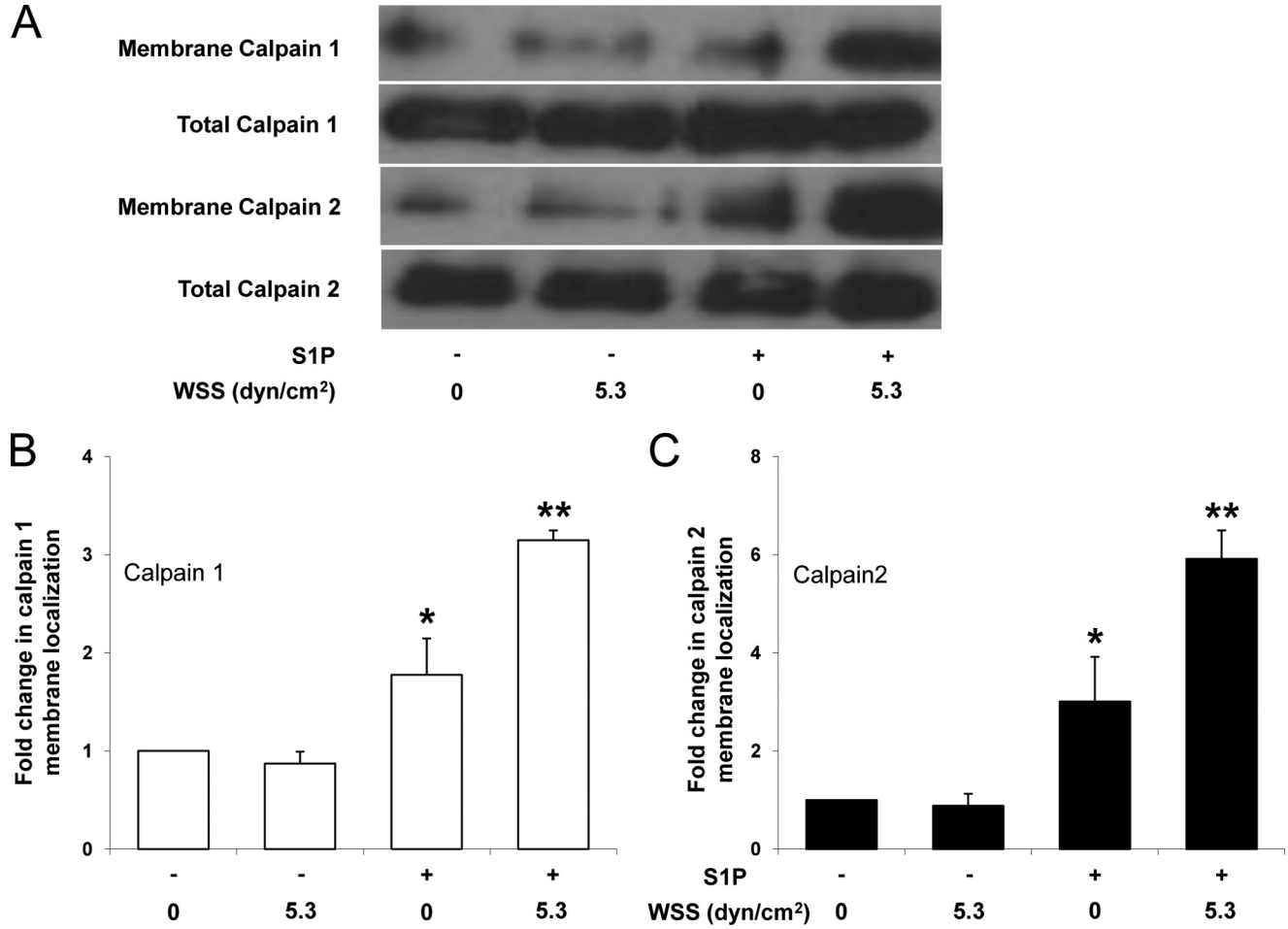

FIGURE 3. **S1P-induced calpain membrane translocation is enhanced by 5.3 dynes/cm^2 WSS.** *A*, ECs were treated with or without S1P (1 μM) for 1 h and then treated with 0 or 5.3 dynes/cm^2 WSS for 2 h. S1P was maintained in the perfusate for the duration of treatment. Cell membranes were isolated as described under "Experimental Procedures." Representative Western blots (*A*) indicate calpain 1 and 2 levels in the membrane (*first* and *third blot*) and total calpain 1 and 2 levels in the starting material (*second* and *fourth blot*). *B* and *C*, intensity values in blots were quantified by densitometric analysis and normalized to total levels in starting material for three independent experiments. Data are presented as fold change in band intensity normalized to 0 S1P and 0 WSS (mean ± S.D.) for calpain 1 (*B*) and calpain 2 (*C*). *, $p < 0.05$ and **, $p < 0.01$ *versus* no S1P and no WSS treatment. *dyn*, dynes.

analysis of variance followed by post hoc pairwise comparison testing using Tukey's method. Two-way analysis of variance was performed when appropriate to determine the effects of time and WSS magnitude on invasion responses.

RESULTS

Calpains Are Required for S1P- and WSS-induced EC Invasion in Three-dimensional Collagen Matrices—We demonstrated previously that S1P and 5.3 dynes/cm^2 WSS combined to induce greater EC invasion than either stimulus applied alone (23). Calpain 1 (μ-calpain) and calpain 2 (m-calpain) are the two major isoforms of calpain. To test for a functional requirement for calpains in WSS+S1P-induced EC invasion responses, pharmacological inhibitors of calpains were tested. ECs were stimulated with S1P and 5.3 dynes/cm^2 WSS in the presence of vehicle control, ALLN, or calpain inhibitor III, which inhibit calpains 1 and 2. Invasion responses were noticeably impaired in the presence of ALLN and calpain inhibitor III (Fig. 1*A*). Photographs of invading structures are shown in supplemental Fig. 1. These findings support the hypothesis that calpains are required for EC invasion responses stimulated by WSS and S1P.

To confirm the results obtained using these pharmacological inhibitors, gene silencing studies using recombinant lentiviruses delivering shRNA directed to calpain 1, calpain 2, β2 microglobulin control, and non-treated cells (HUVEC) were tested. Cross-sectional images illustrate reduced invasion responses (Fig. 1*B*), and this is supported by quantification of invading EC density (Fig. 1*C*). Consistent with the results using calpain antagonists, treatment with either shRNA directed to calpain 1 or calpain 2 blocked invasion responses. In all experiments, cells treated with shRNA directed to β2 microglobulin controls invaded to a comparable extent as non-transfected HUVEC. Selective knockdown of the appropriate calpain isoform with each shRNA was successfully confirmed by Western blot analyses (Fig. 1*D*) and quantified by densitometry (Fig. 1, *E* and *F*). Multiple shRNA sequences that targeted calpain 1 and calpain 2 were delivered to ECs to rule out off-target effects of RNA silencing treatments (supplemental Fig. 2). These results reaffirm that both calpain isoforms are required for S1P and WSS-induced EC invasion in three-dimensional collagen matrices.

Calpains Are Activated during S1P- and WSS-induced Invasion—To determine whether S1P or WSS activate calpains, ECs cultured on three-dimensional collagen matrices contain-

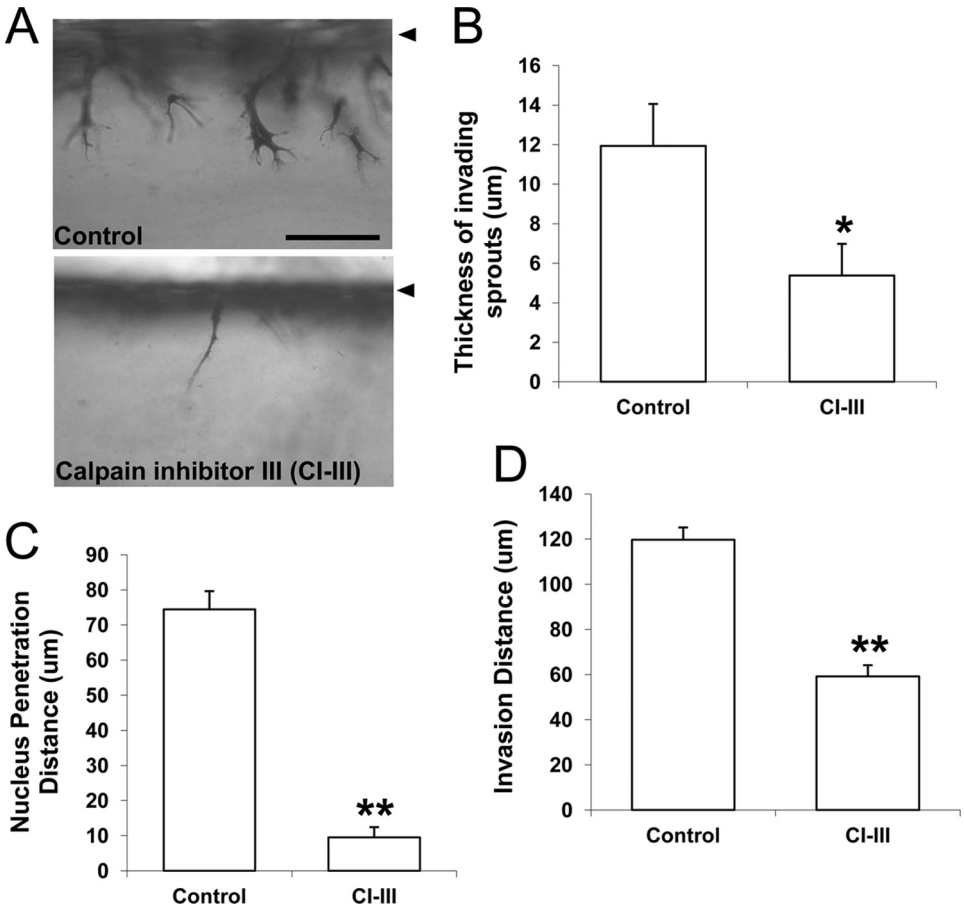

FIGURE 4. **Calpain blockade significantly altered sprout morphology.** *A*, representative photographs of cell invasion responses after 18 h of exposure to 1 μM S1P and 5.3 dynes/cm^2 WSS in the absence (*top*) and presence (*bottom*) of 50 μM calpain inhibitor III (*CI-III*). The thickness of invading sprouts (*B*), the nucleus penetration distance (*C*), and overall invasion distance (*D*) were quantified ($n = 50$ cells from three individual experiments). Data shown are mean values ± S.D.; *, $p < 0.05$ and **, $p < 0.01$ *versus* control. *Scale bar*, 100 μm. *Arrowhead* indicates original monolayer.

ing or lacking S1P (1 μM) were treated with or without 5.3 dynes/cm^2 WSS. Either WSS or S1P applied alone significantly increased calpain activation compared with untreated ECs (Fig. 2*A*). In addition, combined S1P and WSS treatment induced even greater calpain activation. Thus, S1P synergized with 5.3 dynes/cm^2 WSS to activate calpains. The extent of cell invasion was also highest following combined treatment with S1P and 5.3 dynes/cm^2 WSS (Fig. 2*B*), which is consistent with our previous study (23). We next determined the effect of the magnitude of WSS on calpain activation in three-dimensional collagen matrices containing S1P (Fig. 2*C*). 5.3 dynes/cm^2 WSS induced significantly higher calpain activation compared with 0.12 and 12 dynes/cm^2 WSS. In addition, S1P combined with 5.3 dynes/cm^2 WSS more effectively induced invasion than 0.12 and 12 dynes/cm^2 WSS (Fig. 2*D*).

S1P and 5.3 Dynes/cm^2 Preferentially Enhance Calpain Membrane Localization—The results above indicate calpain is necessary for normal invasion in response to WSS and S1P but that overall calpain activation levels do not exclusively explain invasion responses. Calpain activation is often associated with translocation to the membrane that is facilitated by hydrophobic interactions with the lipid bilayer (54, 55). Thus, we next determined whether S1P and 5.3 dynes/cm^2 WSS stimulated calpain membrane translocation. ECs were treated with nothing (control), 5.3 dynes/cm^2 WSS alone, S1P alone, or S1P together with 5.3 dynes/cm^2 WSS. Following each treatment, membrane fractions were isolated and analyzed for levels of calpain (Fig. 3). Quantification of calpain 1 and 2 membrane localization is shown in Fig. 3, *B* and *C*, where calpain intensity in the membrane fraction was normalized to the total levels of calpains in the starting material. These results indicate that combined treatment with S1P and 5.3 dynes/cm^2 WSS resulted in the highest levels of endogenous calpain 1 and 2 detected in membrane isolates. Thus, the combination of S1P and 5.3 dynes/cm^2 WSS enhanced calpain 1 and 2 membrane translocation compared with other treatments and maximal membrane localization of calpains 1 and 2 correlated with increased invasion responses (as shown in Fig. 2*B*).

Calpain Activation Regulates MT1-MMP—We next quantified changes in cell morphology following calpain inhibition. Compared with control cultures, calpain inhibition resulted in extremely thin invading structures (Fig. 4*A*; supplemental Fig. 1), suggesting a possible defect in matrix proteolysis. MT1-MMP plays a key role in matrix proteolysis and regulates angiogenic sprouting events (38, 41, 40, 56). Calpain inhibition significantly attenuated invading sprout thickness (Fig. 4*B*), nucleus penetration distance (Fig. 4*C*), and invasion distance (Fig. 4*D*). These results indicate that the cells with attenuated calpain activity can send thin processes into the matrix, but their nuclei cannot penetrate into the dense collagen three-dimensional

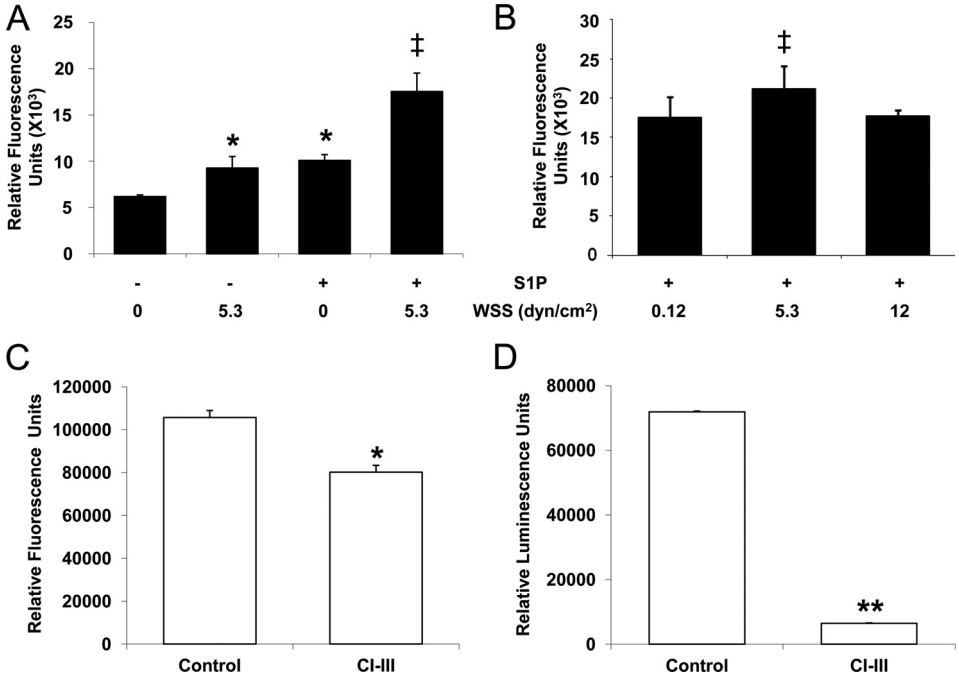

FIGURE 5. **S1P and 5.3 dynes/cm² WSS synergistically activate MT1-MMP.** ECs were subjected to the indicated magnitudes of WSS in the absence or presence of 1 μM S1P for 3 h. *A–C*, MT1-MMP activity was measured using the SensoLyte™ 520 MMP-14 protease assay kit as described under "Experimental Procedures." MT1-MMP (*C*) and calpain (*D*) activation were measured in ECs subjected to 5.3 dynes/cm² WSS+S1P in the presence and absence of the calpain inhibitor III (*CI-III*; 50 μM). Each data point was derived by averaging results of three independent experiments. In each experiment, triplicate wells were established. *, $p < 0.05$ and **, $p < 0.01$ *versus* no S1P and no WSS or control treatment; ‡, $p < 0.05$ *versus* all others. *dyn*, dynes.

matrix. Altogether, impaired morphological responses resulting from calpain inhibition suggest that calpain may regulate MT1-MMP during S1P- and WSS-induced sprouting.

We next quantified MT1-MMP activation in three-dimensional cultures treated with S1P and WSS. S1P or 5.3 dynes/cm² WSS applied alone each increased MT1-MMP activity compared with no treatment (Fig. 5*A*). A further increase in MT1-MMP activity was observed with S1P and WSS combined (Fig. 5*A*). S1P combined with 5.3 dynes/cm² WSS also elicited greater MT1-MMP activation than WSS magnitudes of 0.12 and 12 dynes/cm² (Fig. 5*B*).

MT1-MMP activation was at least partially calpain-dependent as treatment with calpain inhibitor III slightly reduced MT1-MMP activation levels (Fig. 5*C*), while completely inhibiting calpain activation (Fig. 5*D*). As with calpain activity, changes in the levels of MT1-MMP activation did not completely explain the observed invasion responses elicited by S1P and 5.3 dynes/cm² WSS. Thus, we next investigated intracellular localization of MT1-MMP.

S1P can stimulate MT1-MMP translocation to the membrane (57), but the effects of WSS on MT1-MMP localization have not been reported. Experiments were conducted to apply WSS in the presence or absence of S1P. Cells expressing MT1-MMP-GFP were pretreated with 0 or 1 μM S1P and subjected to 0.12, 5.3, and 12 dynes/cm² WSS. In the absence of S1P, almost no localization of MT1-MMP-GFP at the cell periphery was observed at any level of WSS (Fig. 6, *A–C*). In the presence of S1P, 5.3 dynes/cm² WSS elicited much greater localization of MT1-MMP-GFP to the cell periphery (Fig. 6*F*, indicated by *white arrowheads*) than 0.12 or 12 dynes/cm² WSS (Fig. 6, *E* and *G*, respectively). Importantly, MT1-MMP-GFP membrane translocation was almost completely inhibited by blocking calpains with ALLN (Fig. 6*H*) or calpain inhibitor III (data not shown). Interestingly, treatments that did not induce MT1-MMP-GFP membrane translocation resulted in strong perinuclear MT1-MMP-GFP localization (Fig. 6, *black arrowheads*). Quantitative analysis of these images indicates treatment with S1P and 5.3 dynes/cm² WSS significantly increased MT1-MMP-GFP membrane localization compared to other treatments (Fig. 6*I*). Also, calpain inhibition completely inhibited the ability of S1P+5.3 dynes/cm² WSS to induce MT1-MMP-GFP membrane localization. The reliability of MT1-MMP-GFP fusion proteins were confirmed in separate experiments using two independent antibodies directed to MT1-MMP (data not shown).

To confirm that localization of MT1-MMP-GFP in Fig. 6 was an indication of plasma membrane localization, cell fractionation studies were conducted to detect levels of MT1-MMP in isolated membrane fractions (Fig. 7). Fig. 7*A* shows representative blots for ECs treated with nothing, 5.3 dynes/cm² WSS alone, S1P alone, or S1P together with WSS with the quantified results summarized in Fig. 7*C*. Here, MT1-MMP intensity in membrane fractions was normalized to total levels of MT1-MMP. Combined treatment with S1P and WSS resulted in the highest levels of endogenous MT1-MMP detected in membrane isolates (Fig. 7*A*). In addition, significantly higher levels of MT1-MMP were detected following 5.3 dynes/cm² WSS compared with 0.12 or 12 dynes/cm² WSS (Fig. 7, *B* and *D*, respectively), matching invasion responses (Fig. 2, *B* and *D*).

DISCUSSION

Roles for Calpain and WSS in Controlling Angiogenic Switch—Our data show for the first time that S1P and WSS synergistically induce calpain membrane localization to regulate EC inva-

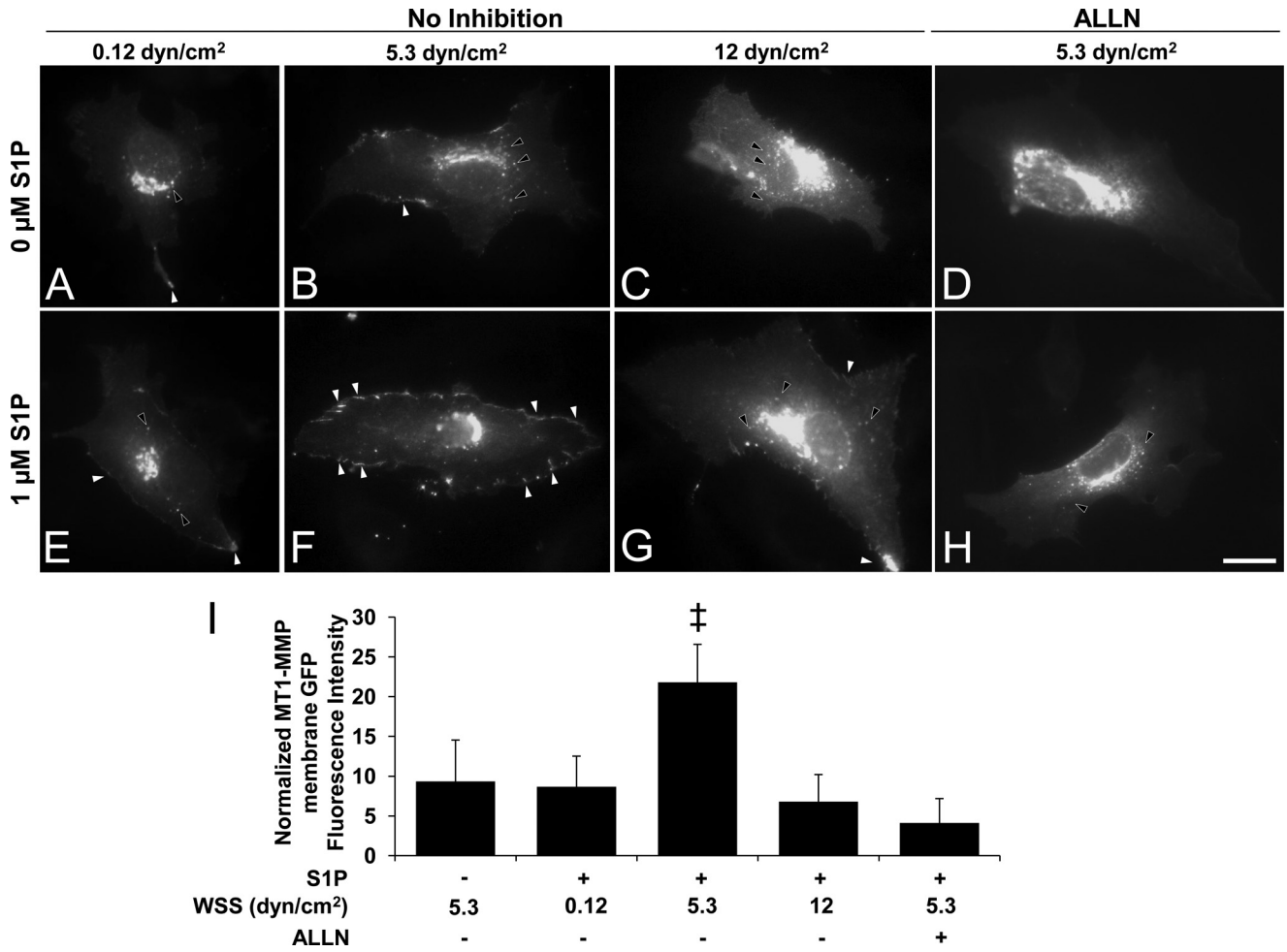

FIGURE 6. **Combined S1P and WSS treatment induced calpain-dependent membrane translocation of MT1-MMP.** ECs transiently transfected with vectors expressing MT1-MMP-GFP chimeras were treated with the indicated magnitudes of WSS in the absence or presence of S1P for 2 h. Transfection efficiency was roughly 20%. In calpain inhibition experiments, cells were pretreated with the calpain inhibitor III (50 μM) for 1 h prior to S1P and WSS treatments, and the inhibitor was maintained in the perfusion medium. *A–H*, *white arrowheads* indicate MT1-MMP-GFP localization to the cell periphery; *black arrowheads* indicate perinuclear localization. *Scale bar*, 20 μm. *I*, MT1-MMP peripheral GFP fluorescence intensities were quantified as described under "Experimental Procedures;" ‡, $p < 0.05$ *versus* all other treatments. *dyn*, dynes.

sion in three-dimensional collagen matrices. Although WSS has been shown previously to activate calpain (24), this is the first study to demonstrate that S1P activates calpain. Furthermore, calpain membrane localization in endothelial cells is stimulated by WSS. Consistent with our previous study (23), we showed a biphasic dependence on WSS magnitude with the greatest invasion observed at 5.3 dynes/cm^2 WSS. This same biphasic WSS dependence was observed for calpain activation and membrane localization in the present study. The current findings suggest that invasion induced by WSS and S1P is partially controlled by activation and membrane translocation of calpains.

There is accumulating evidence that calpain is pivotal in activating the angiogenic switch in ECs. For example, VEGF-induced angiogenesis into Matrigel plugs *in vivo* is blocked by calpain inhibition (26). Our results support previous studies showing calpain is regulated by WSS. Miyazaki and colleagues (24) reported that small interfering RNA against calpain 2, but not against calpain 1, effectively reduced WSS-induced calpain activity in HUVECs. Ariyoshi and colleagues (25) observed increased calpain 2 localization to the membrane in HUVECs in response to 10 dynes/cm^2 WSS, although the effects of other WSS magnitudes were not tested. Miyazaki and colleagues (24) reported that WSS-induced proteolytic activity in HUVECs increased monotonically as WSS magnitude was raised from 0 to 30 dynes/cm^2. In contrast, we observe a biphasic dependence on WSS magnitude. It is not clear why HUVECs show decreased calpain activation and cell invasion at higher WSS, although a number of angiogenic signaling pathways such as hypoxia-inducible factor, endothelial nitric oxide synthesis, and protein kinase B (Akt) activation show a similar dependence on WSS magnitude (66). The differences we observe may be dependent on substrate rigidity because we uniquely apply WSS to endothelial monolayers seeded on three-dimensional collagen matrices and not rigid substrates. We are actively investigating whether substrate rigidity is an important contributing factor.

Calpains Regulate MT1-MMP Following Stimulation by S1P and WSS—MT1-MMP has an indispensible role in angiogenic sprouting into collagen matrices *in vitro* and *in vivo* (38, 58, 59). Although S1P has been shown previously to stimulate MT1-MMP membrane translocation (57), the effects of WSS on

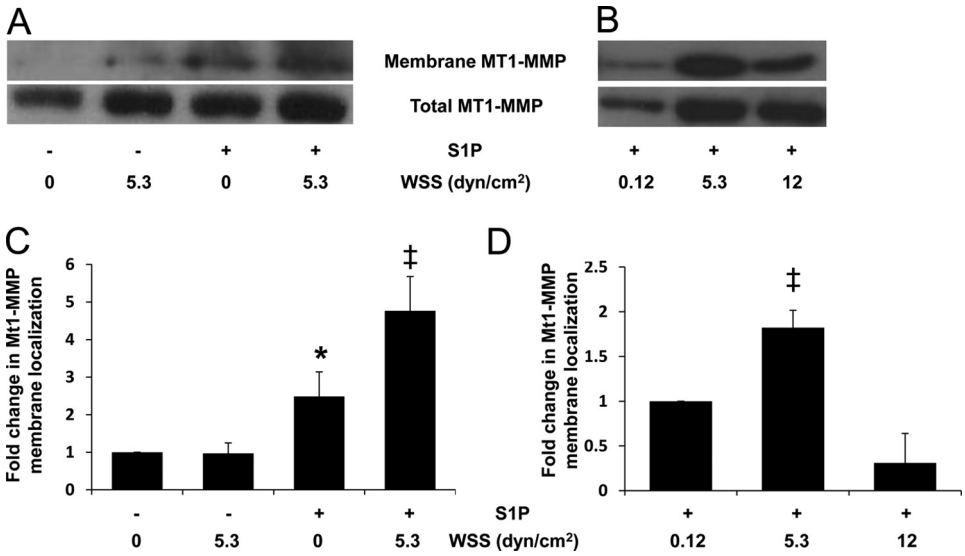

FIGURE 7. **S1P-induced MT1-MMP membrane translocation is enhanced by 5.3 dynes/cm² WSS.** *A* and *C*, ECs were treated in the absence or presence of S1P (1 μM) for 1 h and then subjected to 2 h of 0 or 5.3 dynes/cm^2 WSS. *B* and *D*, ECs were treated with S1P (1 μM) for 1 h and then subjected to 2 h of WSS at the indicated magnitudes. Cell membranes were isolated as described under "Experimental Procedures." Representative Western blots (*A* and *B*) indicate MT1-MMP levels in the membrane (*top blot*) and total cell fractions (*bottom blot*). *C* and *D*, the blots were quantified by densitometric analysis from three independent experiments. Intensity values in blots were normalized to total levels in starting material. Data are presented as fold change in band intensity (mean ± S.D.) normalized to 0 S1P and 0 WSS (*C*) and 0.12 dynes/cm^2 WSS treatment (*D*). *, $p < 0.05$ *versus* no S1P and no WSS treatment; ‡, $p < 0.05$ *versus* all other treatments. *dyn*, dynes.

MT1-MMP membrane translocation have not been reported. Here, we demonstrate for the first time that S1P and 5.3 dynes/cm^2 WSS combine to promote maximal MT1-MMP membrane translocation. Furthermore, calpain activation is required for MT1-MMP membrane translocation and, to a lesser extent, MT1-MMP activation. Calpain inhibition resulted in narrow sprouts and the inability of nuclei to penetrate collagen matrices (*cf.* Fig. 4*A*). However, sprout defects were likely not due simply to inhibition of migration *per se* as sprouts were still fairly long. Rather, these results suggest matrix proteolysis was impaired, supported by reduced movement of relatively large cell nuclei into the matrix. We previously reported that S1P combined with 12 dynes/cm^2 WSS stimulated ECs to extend more rapidly into collagen matrices, albeit with narrower lumens than sprouts from ECs subjected to lower magnitudes of WSS (23). The sprout morphology previously reported with 12 dynes/cm^2 WSS is strikingly similar to that observed here after treatment with calpain inhibitors (*cf.* Fig. 4*A*). Furthermore, 12 dynes/cm^2 WSS-treated samples exhibited significantly lower calpain activation levels and MT1-MMP membrane localization than ECs treated with 5.3 dynes/cm^2 WSS. In our model, S1P combined with 5.3 dynes/cm^2 WSS induced the highest EC invasion responses. Consistent with these results, 5.3 dynes/cm^2 WSS combined with S1P promoted the highest calpain activation and membrane localization, as well as MT1-MMP membrane localization. In addition, calpain inhibition nearly completely blocked MT1-MMP membrane translocation stimulated by WSS combined with S1P. Thus, we find a direct correlation between robust invasion and MT1-MMP membrane localization, which renders the enzyme available to digest collagen fibrils and facilitate invasion responses.

Physiological Implications—Wound healing in skin or other tissues is a complex process. Platelets and immune cells accumulate at sites along damaged blood vessels and release a number of biochemical factors, including VEGF, basic fibroblast growth factor, and S1P (60–63). Additional inflammatory mediators stimulate vasodilatory responses locally that increase WSS by increasing blood flow. These local changes in WSS and S1P may promote EC sprouting into the wound from nearby preexisting vessels. A wide range of WSS levels are used to study mechanotransduction events *in vitro*, with many studies utilizing WSS of 12 dynes/cm^2 or greater. WSS levels in post-capillary venules have been estimated to range from 1 to 5 dynes/cm^2 (12, 20–22, 64). Here, we find S1P synergizes with WSS to induce MT1-MMP and calpain membrane localization, which correlates with EC invasion. A maximal effect is observed at 5.3 dynes/cm^2 WSS, which is comparable with physiological levels in post-capillary venules. The ability of calpains to modulate EC sprouting responses reported here is consistent with recent findings from Senger and colleagues (44, 65) demonstrating that moderate calpain inhibition normalizes pathological angiogenesis. Our data agree with that of Senger and colleagues (44, 65) and support a previously unidentified link between physiological stimuli (*i.e.* S1P +WSS), calpain activation, and control of MT1-MMP membrane localization.

In summary, these results provide a novel molecular mechanism of angiogenic sprout initiation induced by biochemical and mechanical stimuli, namely S1P and WSS. Altogether, these data demonstrate a requirement for calpain in directing MT1-MMP membrane localization in response to stimulation with S1P and 5.3 dynes/cm^2 WSS. This observation is significant in that these conditions optimally stimulate EC sprouting responses in three-dimensional collagen matrices. The regulation of this pathway may underlie vascular remodeling and angiogenic events in a variety of scenarios, including embryonic development, wound healing, and tumor angiogenesis, where

biochemical and mechanical cues initiate new blood vessel growth.

Acknowledgments—We thank Dr. James Moore for providing equipment and Adriana Mendoza for maintenance of endothelial cultures.

REFERENCES

1. Folkman, J., and D'Amore, P. A. (1996) *Cell* **87,** 1153–1155
2. Carmeliet, P. (2003) *Nat. Rev. Genet.* **4,** 710–720
3. Carmeliet, P. (2003) *Nat. Med.* **9,** 653–660
4. Carmeliet, P. (2004) *J. Intern. Med.* **255,** 538–561
5. Davis, G. E., Bayless, K. J., and Mavila, A. (2002) *Anat. Rec.* **268,** 252–275
6. Carmeliet, P., and Collen, D. (2000) *Ann. N.Y. Acad. Sci.* **902,** 249–262
7. English, D., Garcia, J. G., and Brindley, D. N. (2001) *Cardiovasc. Res.* **49,** 588–599
8. Hla, T. (2004) *Semin. Cell Dev. Biol.* **15,** 513–520
9. Nerem, R. M. (1993) *J. Biomech. Eng.* **115,** 510–514
10. Takahashi, M., Ishida, T., Traub, O., Corson, M. A., and Berk, B. C. (1997) *J. Vasc. Res.* **34,** 212–219
11. Clark, E., Hitschler, W., Kirby-Smith, H., Rex, R., and Smith, J. (1931) *Anat. Rec.* **50,** 129–167
12. Ichioka, S., Shibata, M., Kosaki, K., Sato, Y., Harii, K., and Kamiya, A. (1997) *J. Surg. Res.* **72,** 29–35
13. Lucitti, J. L., Jones, E. A., Huang, C., Chen, J., Fraser, S. E., and Dickinson, M. E. (2007) *Development* **134,** 3317–3326
14. Clark, E. (1918) *Am. J. Anat.* **23,** 37–88
15. Nasu, R., Kimura, H., Akagi, K., Murata, T., and Tanaka, Y. (1999) *Br. J. Cancer* **79,** 780–786
16. Hogers, B., DeRuiter, M. C., Gittenberger-de Groot, A. C., and Poelmann, R. E. (1997) *Circ. Res.* **80,** 473–481
17. Hove, J. R., Köster, R. W., Forouhar, A. S., Acevedo-Bolton, G., Fraser, S. E., and Gharib, M. (2003) *Nature* **421,** 172–177
18. Isogai, S., Lawson, N. D., Torrealday, S., Horiguchi, M., and Weinstein, B. M. (2003) *Development* **130,** 5281–5290
19. Olson, E. N., and Srivastava, D. (1996) *Science* **272,** 671–676
20. Kim, M. B., and Sarelius, I. H. (2003) *Microcirculation* **10,** 167–178
21. Boisseau, M. R. (2005) *Clin. Hemorheol. Microcirc.* **33,** 201–207
22. Jones, E. A., Baron, M. H., Fraser, S. E., and Dickinson, M. E. (2004) *Am. J. Physiol. Heart Circ. Physiol.* **287,** H1561–1569
23. Kang, H., Bayless, K. J., and Kaunas, R. (2008) *Am. J. Physiol. Heart Circ. Physiol.* **295,** H2087–2097
24. Miyazaki, T., Honda, K., and Ohata, H. (2007) *Am. J. Physiol. Cell Physiol.* **293,** C1216–1225
25. Ariyoshi, H., Yoshikawa, N., Aono, Y., Tsuji, Y., Ueda, A., Tokunaga, M., Sakon, M., and Monden, M. (2001) *J. Cell. Biochem.* **81,** 184–192
26. Su, Y., Cui, Z., Li, Z., and Block, E. R. (2006) *FASEB J.* **20,** 1443–1451
27. Carragher, N. O., Fonseca, B. D., and Frame, M. C. (2004) *Neoplasia* **6,** 53–73
28. Franco, S., Perrin, B., and Huttenlocher, A. (2004) *Exp. Cell Res.* **299,** 179–187
29. Wells, A., Huttenlocher, A., and Lauffenburger, D. A. (2005) *Int. Rev. Cytol.* **245,** 1–16
30. Butcher, J. T., Penrod, A. M., García, A. J., and Nerem, R. M. (2004) *Arterioscler. Thromb. Vasc. Biol.* **24,** 1429–1434
31. Tamada, Y., Fukiage, C., Boyle, D. L., Azuma, M., and Shearer, T. R. (2000) *J. Ocul. Pharmacol. Ther.* **16,** 271–283
32. Flevaris, P., Stojanovic, A., Gong, H., Chishti, A., Welch, E., and Du, X. (2007) *J. Cell Biol.* **179,** 553–565
33. Potter, D. A., Tirnauer, J. S., Janssen, R., Croall, D. E., Hughes, C. N., Fiacco, K. A., Mier, J. W., Maki, M., and Herman, I. M. (1998) *J. Cell Biol.* **141,** 647–662
34. Cortesio, C. L., Chan, K. T., Perrin, B. J., Burton, N. O., Zhang, S., Zhang, Z. Y., and Huttenlocher, A. (2008) *J. Cell Biol.* **180,** 957–971
35. Calle, Y., Carragher, N. O., Thrasher, A. J., and Jones, G. E. (2006) *J. Cell Sci.* **119,** 2375–2385
36. Marzia, M., Chiusaroli, R., Neff, L., Kim, N. Y., Chishti, A. H., Baron, R., and Horne, W. C. (2006) *J. Biol. Chem.* **281,** 9745–9754
37. Linder, S., and Aepfelbacher, M. (2003) *Trends Cell Biol.* **13,** 376–385
38. Chun, T. H., Sabeh, F., Ota, I., Murphy, H., McDonagh, K. T., Holmbeck, K., Birkedal-Hansen, H., Allen, E. D., and Weiss, S. J. (2004) *J. Cell Biol.* **167,** 757–767
39. Hotary, K., Allen, E., Punturieri, A., Yana, I., and Weiss, S. J. (2000) *J. Cell Biol.* **149,** 1309–1323
40. Hiraoka, N., Allen, E., Apel, I. J., Gyetko, M. R., and Weiss, S. J. (1998) *Cell* **95,** 365–377
41. Saunders, W. B., Bohnsack, B. L., Faske, J. B., Anthis, N. J., Bayless, K. J., Hirschi, K. K., and Davis, G. E. (2006) *J. Cell Biol.* **175,** 179–191
42. Yana, I., Sagara, H., Takaki, S., Takatsu, K., Nakamura, K., Nakao, K., Katsuki, M., Taniguchi, S., Aoki, T., Sato, H., Weiss, S. J., and Seiki, M. (2007) *J. Cell Sci.* **120,** 1607–1614
43. Nisato, R. E., Hosseini, G., Sirrenberg, C., Butler, G. S., Crabbe, T., Docherty, A. J., Wiesner, M., Murphy, G., Overall, C. M., Goodman, S. L., and Pepper, M. S. (2005) *Cancer Res.* **65,** 9377–9387
44. Hoang, M. V., Smith, L. E., and Senger, D. R. (2011) *Biochim. Biophys. Acta.* **1812,** 549–557
45. Holmbeck, K., Bianco, P., Caterina, J., Yamada, S., Kromer, M., Kuznetsov, S. A., Mankani, M., Robey, P. G., Poole, A. R., Pidoux, I., Ward, J. M., and Birkedal-Hansen, H. (1999) *Cell* **99,** 81–92
46. Zhou, Z., Apte, S. S., Soininen, R., Cao, R., Baaklini, G. Y., Rauser, R. W., Wang, J., Cao, Y., and Tryggvason, K. (2000) *Proc. Natl. Acad. Sci. U.S.A.* **97,** 4052–4057
47. Langlois, S., Nyalendo, C., Di Tomasso, G., Labrecque, L., Roghi, C., Murphy, G., Gingras, D., and Béliveau, R. (2007) *Mol. Cancer Res.* **5,** 569–583
48. Nyalendo, C., Michaud, M., Beaulieu, E., Roghi, C., Murphy, G., Gingras, D., and Béliveau, R. (2007) *J. Biol. Chem.* **282,** 15690–15699
49. Bayless, K. J., Kwak, H. I., and Su, S. C. (2009) *Nat. Protoc.* **4,** 1888–1898
50. Bornstein, M. B. (1958) *Lab. Invest.* **7,** 134–137
51. Bayless, K. J., and Davis, G. E. (2003) *Biochem. Biophys. Res. Commun.* **312,** 903–913
52. Davis, G. E., and Camarillo, C. W. (1996) *Exp. Cell Res.* **224,** 39–51
53. Su, S. C., Mendoza, E. A., Kwak, H. I., and Bayless, K. J. (2008) *Am. J. Physiol. Cell Physiol.* **295,** C1215–1229
54. Hood, J. L., Brooks, W. H., and Roszman, T. L. (2006) *Bioessays* **28,** 850–859
55. Hood, J. L., Logan, B. B., Sinai, A. P., Brooks, W. H., and Roszman, T. L. (2003) *Biochem. Biophys. Res. Commun.* **310,** 1200–1212
56. Hotary, K. B., Allen, E. D., Brooks, P. C., Datta, N. S., Long, M. W., and Weiss, S. J. (2003) *Cell* **114,** 33–45
57. Langlois, S., Gingras, D., and Béliveau, R. (2004) *Blood* **103,** 3020–3028
58. Pepper, M. S. (2001) *Arterioscler. Thromb. Vasc. Biol.* **21,** 1104–1117
59. Stratman, A. N., Saunders, W. B., Sacharidou, A., Koh, W., Fisher, K. E., Zawieja, D. C., Davis, M. J., and Davis, G. E. (2009) *Blood* **114,** 237–247
60. Möhle, R., Green, D., Moore, M. A., Nachman, R. L., and Rafii, S. (1997) *Proc. Natl. Acad. Sci. U.S.A.* **94,** 663–668
61. Martin, P., and Leibovich, S. J. (2005) *Trends Cell Biol.* **15,** 599–607
62. Martyré, M. C., Le Bousse-Kerdiles, M. C., Romquin, N., Chevillard, S., Praloran, V., Demory, J. L., and Dupriez, B. (1997) *Br. J. Haematol.* **97,** 441–448
63. Yatomi, Y., Igarashi, Y., Yang, L., Hisano, N., Qi, R., Asazuma, N., Satoh, K., Ozaki, Y., and Kume, S. (1997) *J. Biochem.* **121,** 969–973
64. Koutsiaris, A. G., Tachmitzi, S. V., Batis, N., Kotoula, M. G., Karabatsas, C. H., Tsironi, E., and Chatzoulis, D. Z. (2007) *Biorheology.* **44,** 375–386
65. Hoang, M. V., Nagy, J. A., Fox, J. E., and Senger, D. R. (2010) *PLoS One* **5,** e13612
66. Kaunas, R., Kang, H., and Bayless, K. J. (2011) *Cell. Mol. Bioeng.*, in press